

Green synthesis and characterization of silver and iron nanoparticles using *Nerium oleander* extracts and their antibacterial and anticancer activities

Shalima Shawuti ¹, Chasan Bairam ², Ahmet Beyatlı ³, İshak Afşin Kariper ⁴, Isık Neslişah Korkut ¹, Zerrin Aktaş ⁵, Mustafa Oral Öncül ⁶, Serap Erdem Kuruca ¹

¹ Department of Physiology, Faculty of Medicine, Istanbul University, Turgut Özal Millet str., 34093 Istanbul, Turkey

² Renewable Energy and Oxide Hybrid Systems Laboratory, Department of Physic, Faculty of Science, Istanbul University, Şehzadebaşı str., 34134 Istanbul, Turkey

³ Department of Medicinal and Aromatic Plants, Hamidiye Vocational School of Health Services, University of Health Sciences, Tıbbiye str. 38, 34668 Istanbul, Turkey

⁴ Faculty of Education, Erciyes University, Yenidoğan Mahallesi, Turhan Baytop Sokak str. 1, 38280 Kayseri, Turkey

⁵ Department of Microbiology, Faculty of Medicine, Istanbul University, Turgut Özal Millet str., 34093 Istanbul, Turkey

⁶ Department of Infectious Diseases, Faculty of Medicine, Istanbul University, Turgut Özal Millet str., 34093 Istanbul, Turkey

Received: 19.08.2021 | Accepted: 21.11.2021 | Published online: 28.11.2021

Abstract

Medicinal plants can be used as reducing agents in the preparation of metal nanoparticles by green synthesis because of the chemotherapeutic and anti-infectious properties of natural compounds. Therefore, this paper reports the green synthesis of silver and iron nanoparticles from leaf and flower extracts of *Nerium oleander* and their capacity as anticancer and antimicrobial agents. Nanoparticle manufacturing and structural characterization of silver and iron nanoparticles are reported. The formation of nanoparticles is characterized by scanning electron microscopy with energy dispersive X-ray spectroscopy, UV-Vis and Fourier transform infrared (FTIR) spectroscopy. Nanoparticles formation was also investigated the surface charge, particle size, and distribution using zeta sizer analysis by DLS. Green synthesis of silver and iron nanoparticles using *N. oleander* showed different levels of selective cytotoxicity against K562 (human chronic myeloid leukemia cells) in low concentrations and were not cytotoxic to the HUVEC (human umbilical vein endothelial cells) in the same concentrations. Silver nanoparticles showed antibacterial activity against multidrug pathogens, while iron nanoparticles failed to show such activity. Results of the present research demonstrate the potential use of green synthesized nanoparticles in various biomedicine and pharmaceuticals fields in the future.

Keywords: *Nerium oleander*, green synthesis, Ag-nanoparticles, Fe-nanoparticles, cellular cytotoxicity, antibacterial effect

Authors' contributions: Shalima Shawuti is principle investigator. Chasan Bairam is master student who carried out XRD and UV-Vis analysis. Ahmet Beyatlı is researcher collect and prepare leaf extract; also did phytochemical screening test, İshak Afşin Kariper is researcher who perform SEM and DLS analysis. Isık Neslişah Korkut is master student who investigate the cytotoxic test, Zerrin Aktaş and Mustafa Oral Öncül are collaborators who perform antibacterial tests and write evaluation on those part. Finally, Serap Erdem Kuruca is co-principle investigator and supervisor.

Funding: This work was also supported by the Scientific Research Projects Coordination Unit of Istanbul University.

Competing Interests: We wish to confirm that there are no known conflicts of interest with this publication and there has been no significant financial support for this work that could have influenced its outcome. We confirm that the manuscript has been read and approved by all named authors and that there are no other persons who satisfied the criteria for authorship but are not listed. We further confirm that the order of authors listed in the manuscript has been approved by all of us.

Introduction

Nanoparticles (NPs) are synthesized generally by expensive chemical synthesis methods that require the use of toxic chemicals. Thus, using biomolecules (i.e., bacteria, fungi, or plants) for NPs synthesis became a common method in past years that is safe, low-cost, and ecofriendly. Different plant extracts can be act as safe natural capping, reducing, and stabilizing agents without being a source of thermal or chemical hazards (Fedlheim & Foss, 2001; Arya, 2010). Nanoparticles formation can be a glimmer of hope for the production of drugs that can be used against infectious diseases and cancer.

Nerium oleander L. (Apocynaceae), grown in wetlands of the Mediterranean region, can be seen wild as well cultivated as an ornamental plant in parks and gardens. It is an evergreen shrub with pink and white flowers (Baytop, 1999). The plant grows up to 2–6 m tall. The leaves are in pairs or whorls of three, thick and leathery, dark-green, narrowly lanceolate, 5–21 cm long, and with an entire margin. Flowers develop in clusters at the end of branches, the diameter of each flower range about 2.5–5 cm with a deeply 5-lobed fringed corolla around the central corolla tube. The fruit is a long narrow capsule 5–23 cm long, which splits open at maturity to release numerous downy seeds (Baytop, 1999; Kiran & Prasad, 2014).

The leaves and flowers of *N. oleander* used in folkloric medicine among people in Turkey for rheumatism and urticaria (Bulut & Tuzlaci, 2013; Sağıroğlu et al., 2013). The latex of plant used for eczema (Gürdal & Kültür, 2013). Over the world, different parts of this plant are used traditionally for the treatment of various human ailments, including dermatitis, eczema, herpes, skin cancer, asthma, epilepsy, malaria, and tumors (Santhi, 2011). *Nerium oleander* is considered one of the most poisonous plants in the world which leads annually to the death of many people and animals (Rubini et al., 2019). This toxicity is due to toxins like oleandrin, oleandrogenin, and nerine, which belong to cardiac glycosides (Al-Badrani et al., 2008; Zibbu & Batra, 2010). In addition, the plant contains terpenoids and steroids (Santhi, 2011).

Despite the toxicity of plant, different scientific studies conducted on various parts of

N. oleander showed its antibacterial (Chauhan et al., 2017), hepatoprotective and antioxidant (Singhal & Gupta, 2012), antiproliferative (Wong et al., 2011), antidiabetic (Sikarwar et al., 2009), anti-inflammatory (Erdemoglu et al., 2003), and anticancer (Pathak et al., 2000; Turan et al., 2006) activities. This study was aimed to synthesize Ag and Fe nanoparticles using leaves and flowers of *N. oleander* and then evaluate its antibacterial and anticancer activity against human chronic myeloid leukemia cell line.

Material and methods

Chemicals and reagents

An anhydrous FeCl_3 with 98% purity (Merck, Germany), AgNO_3 with 99.5% purity (Sigma-Aldrich, USA) were used as metal sources. Dulbecco's modified Eagle medium (DMEM) and fetal bovine serum (FBS) (Gibco, UK) and MTT (3-[4,5-dimethylthiazol-2-yl]-2,4-diphenyltetrazolium bromide) were applied. All reagents used were of analytical grades.

Plant material

Nerium oleander leaves and flowers were collected from Servetiye Village, Sakarya Province, Turkey in June 2020. Plant was identified at the Herbarium of Faculty of Pharmacy, Istanbul University (voucher number – ISTE-117270).

Preparation of extracts

Collected dried leaves and flowers of *N. oleander* were washed thoroughly (three times) in distilled water and homogenized using a mortar and pestle. The shade dried leaves and flowers of *N. oleander* were powdered and then 10 g of both leaves and flowers were suspended in 100 ml of distilled water. Mixtures stirred for 20 min at 60 °C, then allowed to cool at room temperature, and then filtered using a Whatman no. 42 filter paper and centrifuged at $\times 2000$ rpm for 20 min (Byrne et al., 2016). The extracts prepared were then transferred to a sterile container. The extracts were stored at 4 °C and freshly used.

Preliminary phytochemicals screening

Nerium oleander extracts were subjected to qualitative screening for the presence

Table 1. pH values of the NO-AgNPs and NO-FeNPs. The pH values were measured on leaf extract, after mixing with a metal salt, and after 24 hours of mixing.

Formation	Extract pH	Extract+Metal NO ₃ (0h)	Extract+metal NO ₃ (24h)
NOL-AgNPs	6.78	6.56	4.21
NOF-AgNPs	5.42	6.12	3.74
NOL-FeNPs	6.78	2.32	2.17
NOF-FeNPs	5.42	2.33	2.25

of various phytochemicals using standard procedures (Tyler, 1993; Harborne, 1998).

Preparation of *Nerium oleander* silver nanoparticles (NO-AgNPs)

2.5 mL from the leaf (L) and flower (F) extract solutions were taken and mixed with 1 mM AgNO₃ in 47.5 mL deionized water and a solution of 50 mL in amount was obtained. The pH values of crude leaf and flower extracts, pH values of samples just after mixing with AgNO₃ metal source and after 24 h were measured (Table 1). The pH of the prepared AgNO₃ solution was 5.28.

Preparation of *Nerium oleander* iron nanoparticles (NO-FeNPs)

Same sample preparation steps were followed for iron nanoparticles. Briefly, 5 mL from the leaf and flower extract solutions was taken and mixed with 0.2 M FeCl₃ in 45 mL deionized water and a solution of 50 mL in amount was obtained. The pH values of crude leaf and flower extracts, pH values of samples just after mixing with FeCl₃ and after 24 h were measured (Table 1). The pH of the prepared FeCl₃ solution was 2.25.

Characterization of *Nerium oleander* AgNPs and FeNPs

The synthesized nanoparticles were characterized through a UV-Vis spectrophotometer Shimadzu 2600. The reduction of nanoparticles was monitored by UV-spectrophotometer range of absorbance from 250–480 nm. The crystalline structures of the green-synthesized *N. oleander* (AgNP) and (FeNP) were examined by XRD Rigaku Flex 600 (600 models, with $\lambda=1.5406$ and with a step size of 0.02 Å) at speed of 3 ° min⁻¹. Particle size and zeta potential were measured by Malvern Nano ZS. Morphology and elemental metal mapping were recorded

using a high-resolution scanning electron microscope (SEM, Carl Zeiss Ultra Plus Gemini Fesem) were used to investigate 2D surface morphologies. The composition analyses of the samples were performed by EDX (EDX spectrometer attached to SEM). Fourier transformed infrared (FTIR) analyses were carried out on a liquid sample with Bruker Alpha FTIR spectrometer in the range from 4000–500 cm⁻¹. The device had a DTGS detector and ten scans were conducted for each spectrum with resolution four.

Cytotoxic assay

K562 (human chronic myeloid leukemia cells) and HUVEC (human umbilical vein endothelial cells) cell lines were obtained from American Type Culture Collection (ATCC). Cells were cultured in DMEM with 10% FBS and 1% penicillin/streptomycin in a 5% CO₂ humidified incubator, maintained at 37 °C. First, *N. oleander* nanoparticles were sterilized and diluted with DMEM to prepare four different dilutions which are 1, 1/2, 1/5, and 1/10. MTT assays were performed in 96-well plates. The plant extract and metal concentrations found in these nanoparticle dilutions are also shown in Table 2. K562 cells (about 105 cells per well) were seeded and incubated for 72 h. Then, supernatants were removed, and 10 µL (MTT – 5 mg/mL) solution was added to each well. Following incubation at 37 °C for 3.5 h and kept dark in a humidified atmosphere at 5% CO₂ in the air. Subsequently, the supernatant was discarded, and the precipitated formazan was dissolved in dimethyl sulfoxide (100 µL per well). The optical density of the solution was evaluated using a microplate spectrophotometer at a wavelength of 570 nm (Mosmann, 1983). GraphPad Prism was used to calculate cell viability and IC₅₀ values.

Table 2. The nanoparticle dilutions used in cytotoxicity tests.

Dilutions	NOF-Ag	NOL-Ag	NOF-Fe	NOL-Fe
1	500 ug/mL	500 ug/mL	1000 ug/mL	1000 ug/mL
	20 uM/mL	20 uM/mL	1 mM/mL	1 mM/mL
1/2	250 ug/mL	250 ug/mL	500 ug/mL	500 ug/mL
	10 uM/mL	10 uM/mL	0.5 mM/mL	0.5 mM/mL
1/5	100 ug/mL	100 ug/mL	200 ug/mL	200 ug/mL
	4 uM/mL	4 uM/mL	0.02 mM/mL	0.02 mM/mL
1/10	50 ug/mL	50 ug/mL	100 ug/mL	100 ug/mL
	2 uM/mL	2 uM/mL	0.01 mM/mL	0.01 mM/mL

Antibacterial activity

The antibacterial potential was tested against 14 different human pathogenic bacteria including three Gram-negative bacteria (*Escherichia coli* ATCC 35218, clinical isolates of carbapenem-resistant *Klebsiella pneumoniae* (CRKpn) and carbapenem-resistant *E. coli* (CREc)) and 11 Gram-positive bacteria (*Staphylococcus aureus* ATCC 29213 and ATCC 25923, inducible-clindamycin-resistant *S. aureus* (ICRSa) BAA976-1, hetero-resistant *S. aureus* (hVISA), clinical isolates of methicillin-resistant *S. aureus* (MRSA), methicillin-resistant coagulase-negative *S. aureus* (MR-CoNS:2), vancomycin-resistant *Enterococcus faecium* (VREf), *E. faecalis* ATCC 29212 and 51279, and vancomycin susceptible *E. faecalis* (VSEf)). The species were identified by using the Vitek 2 system (bioMerieux Vitek Inc.).

Antibacterial activity was detected by minimum inhibition concentrations (MICs), which were determined by serial microdilution method (MIC ranges - 2.5–0.0012 mg/L for NOL-AgNPs and NOF-AgNPs, and 5.0–0.0024 mM for AgNO₃) following CLSI (2018). Briefly, 100 µL of each concentration were added to a well (96-well microplate) containing 100 µL of Mueller Hinton Broth (MHB) and 10 µL of inoculum (0.5 McFarland; 1.5 × 10⁸ colony forming units/mL). Plates were then incubated at 37 °C for 24 h. Bacterial growth was determined by absorbance at 600 nm.

List of applied abbreviations

ATCC – American Type Culture Collection
 CREc – carbapenem-resistant *Escherichia coli*
 CRKpn – carbapenem-resistant *Klebsiella pneumoniae*

DLS – dynamic light scattering
 DMEM – Dulbecco's modified Eagle medium
 FBS – fetal bovine serum
 FTIR – Fourier transform infrared
 HUVEC – human umbilical vein endothelial cells
 hVISA – heteroresistant *Staphylococcus aureus*
 IC₅₀ – half maximal inhibitory concentration
 ICRSa – inducible clindamycin-resistant *S. aureus*
 K562 – human chronic myeloid leukemia cells
 MIC – minimum inhibition concentrations
 MR-CoNS:2 – methicillin-resistant coagulase-negative *S. aureus*
 MRSA – methicillin-resistant *S. aureus*
 NO – *Nerium oleander*
 NOF – *N. oleander* flowers extract
 NOL – *N. oleander* leaves extract
 NPs – nanoparticles
 SEM – scanning electron microscopy
 UV-Vis – Uv-Vis spectroscopy
 VREf – vancomycin-resistant *Enterococcus faecalis*
 VSEf – vancomycin-susceptible *E. faecalis*
 XRD – X-ray spectroscopy

Results and discussion

Preliminary phytochemicals screening

Qualitative phytochemical analysis of *N. oleander* extracts showed the presence of different active components in the aqueous extracts (Table 3). Previous works on *N. oleander* revealed the presence of alkaloids, flavonoids, glycosides, tannins, terpenoids, and saponins in this plant

Table 3. Preliminary phytochemical screening of leaves and flowers of *Nerium oleander* extract (plus and minus indicate the presence and absence of the chemicals, respectively).

Phytochemicals	Leaves	Flowers
Alkaloids	+	+
Flavonoids	-	+
Saponins	+	+
Terpenoids	-	-
Steroids	-	-
Tannins	+	+
Glycosides	+	+



Figure 1. Synthesis of Ag and Fe nanoparticles exhibit color change. **First row** – solutions fabricated with leaf extracts (1 – NOL-Ag; 2 – NOL-Ag after 24 h; 3 – crude NOL extract; 4 – NOL-Fe; 5 – NOL-Fe after 24 h). **Second row** – solutions fabricated with flower extracts (6 – NOF-Ag; 7 NOF-Ag after 24 h; 8 – crude NOF extract; 9 – NOF-Fe; 10 – NOF-Fe after 24 h).

(Chaudhary et al., 2015; Saranya et al., 2017). The existence of these constituents can be the main reason behind the biological activity.

Synthesis of Fe/Ag NPs by visual inspection

After 24 h of reaction, the reaction solution color changed from light to dark color, which can be seen in Fig. 1. The reduction of Fe^{3+} ions exhibits a dark color due to the excitation of surface plasmon vibration in a metal nanoparticle. Similarly, in the reduction of Ag^+ ions, the solution color change from light pink to light yellow. Visual photo images of the NOF-NPs are not reported due to similarity in colors with NOL-NPs.

SEM and DLS measurement

The scanning electron microscopy (SEM) technique was used to evaluate the morphology and size of the green synthesized NOL-AgNPs. Fig. 2 represents the surface images and DLS size distribution of green synthesized nanoparticles (NO-AgNPs). Specifically, the nanoparticles appear aggregated and spread uniform shapes. Iron nanoparticles seem also spherical with 70 nm average diameters. In another study, silver nanoparticles from *N. oleander* flowers were synthesized (Bharathi & Shanthi, 2017). Silver particles of about 10 μm by SEM analysis are very small compared to ours, but we do not know their effectiveness as authors did not report their bioactivity. Besides, such small particles are not suitable for clinical use as they will be much easier to eliminate by the immune system (Bharathi & Shanthi, 2017).

The zeta potential is an indicator of surface charge potential, which is an important parameter for understanding the stability of nanoparticles in aqueous suspensions. Table 4 summarizes DLS size distribution measurements carried out on green synthesized NPs. For the NOF-FeNPs, the average particle size was 1872 nm with a polydispersity index of 0.69 (zeta potential – +5.3 mV). On the other hand, particle sizes of NOF-AgNPs were found 76 nm size with relatively homogenous distribution (polydispersity index – 0.266, zeta potential – +8.1 mV). Secondly, For the NOL-FeNPs, the average particle size was 609 nm with a polydispersity index of 0.54 (zeta potential – +7.4 mV). On the other hand, particle sizes of NOL-AgNPs were found 93 nm size with relatively homogenous distribution (polydispersity index – 0.364, zeta potential – +8.8 mV). No aggregation of the colloidal was observed for several months. Therefore, it may suggest that all synthesized NOF-NPs and NOL-NPs were highly stable when stored at the required temperature. It was also observed that produced NPs had positively charged on their surface with zeta potential values above 5 mV.

UV spectroscopy

The characterization of silver and iron nanoparticles by UV-spectrophotometer from the range of 350–900 nm was performed to monitor the reduction of metal ions and their

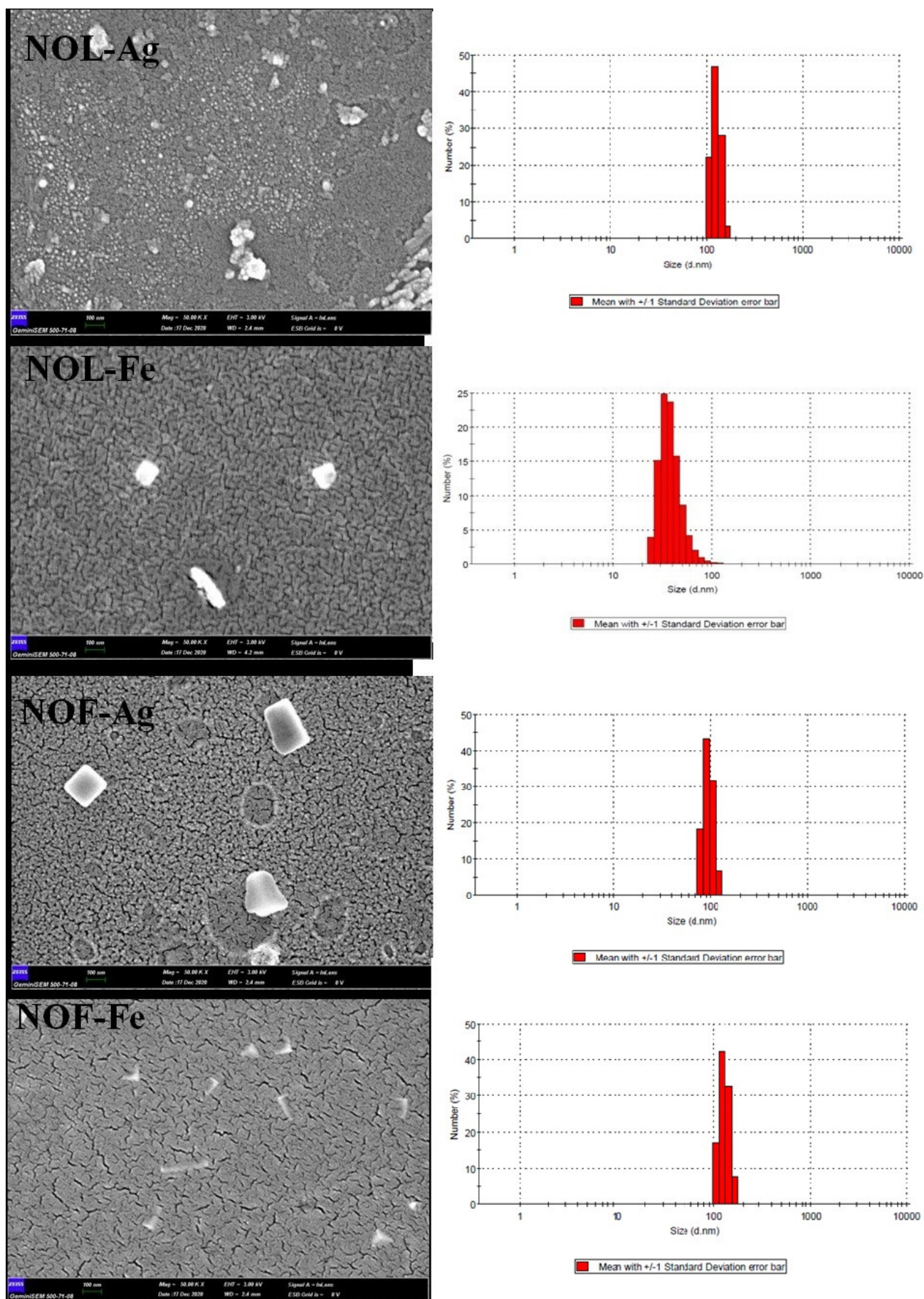


Figure 2. SEM image and DLS size distribution of *Nerium oleander* related NPs. The SEM images were obtained on dried powder samples.

Table 4. The DLS, polydispersity index, and zeta potential of NO-NPs.

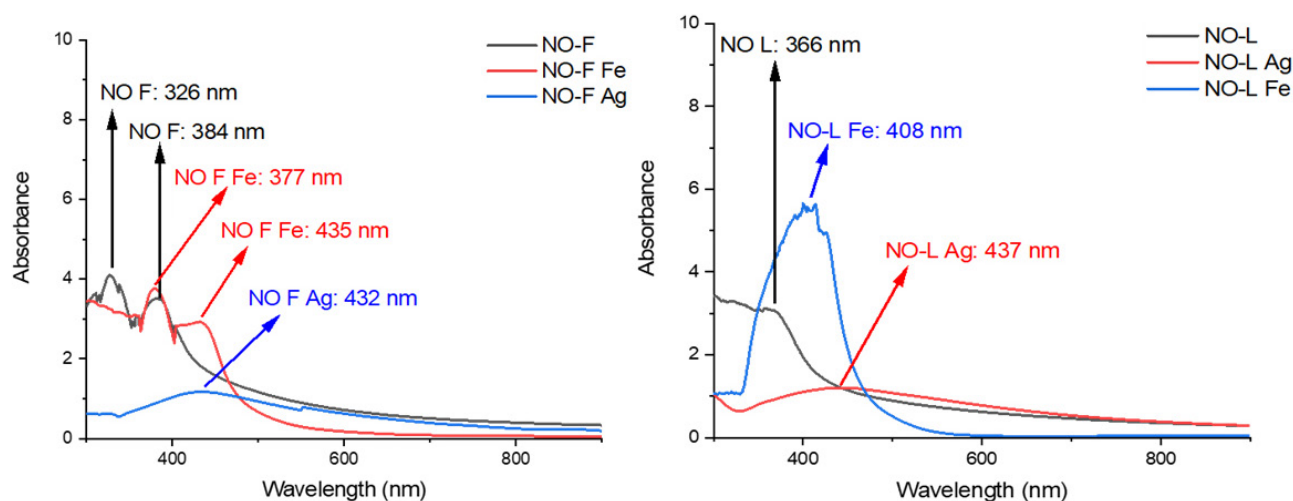
Formation	Average diameter (nm)	Polydispersity index	Zeta potential (mV±SD)
NOF-FeNPs	130.0	0.690	+5.3±9.3
NOF-AgNPs	76.1	0.266	+8.1±0.3
NOL-FeNPs	39.1	0.251	+7.4±0.4
NOL-AgNPs	92.9	0.364	+8.8±0.8

stability. The broad absorption peaks in the range from 326 to 432 nm were represented in Fig. 3. UV-Vis spectra were performed for NO-AgNPs and NO-FeNPs fabricated with leaf and flower extracts. To observe any shift, both crude NOL and NOF were also investigated. The absorption peaks of a plant extract with an organic mixture were not able to record since they are belonging to C-C and C-H electronic transitions (below 250 nm wavelength). The absorption peaks for NOF at 326 and 384 nm wavelengths belong to the $n-\pi^*$ and $\pi-\pi^*$ transitions (Wang et al., 2014). It is because this plant extract contains carbon-carbon double bonds, nitrogen-oxygen bonds, or cyclic aromatic structures. This absorption peak was only seen at 366 nm for NOL. While Ag nanoparticle synthesized with NOF gives an absorption peak at 432 nm as expected. The synthesized Fe NP continued to interact with functional groups in the plant extract, and while a specific 435 nm absorption peak was observed in the region belonging to a typical metal nanoparticle, an absorption peak appeared at 377 nm due to its interaction with functional groups. Another possible

explanation for this phenomenon is that the Fe nanoparticle can be in Fe_2O_3 or Fe_3O_4 structure types (Wang et al., 2014). UV-Vis spectra with the NOL nanoparticles showed much clearer absorption peaks of metal nanoparticles compared to a case in NOF. The Ag NPs absorption peak was observed at 437 nm whereas the Fe NPs was detected at 408 nm.

XRD analysis

The crystalline structures of the green-synthesized NOL-FeNPs, NOF-FeNPs, NOF-AgNPs, and NOF-AgNPs were furtherly examined by XRD analysis. The obtained patterns were demonstrated in Fig. 4 with labeled indices together with two theta values. The obtained diffraction peaks at 2θ values of 23.5° , 26.6° , 35.8° , 39.1° , and 46.2° were assigned to (012), (120), (110), (113) and (202) lattice planes, respectively. Those sets of lattice planes were identical to those reported for standard iron metal. For NOL-FeNPs, the iron nanoparticles are FCC and crystalline (cubic crystalline structure, $a=4.07100 \text{ \AA}$; JCPDS files no. 84-0713 and 04-0783). NO-AgNPs are FCC

**Figure 3.** UV-Vis of NOL and NOF extracts and NO-FeNPs and NO-AgNPs.

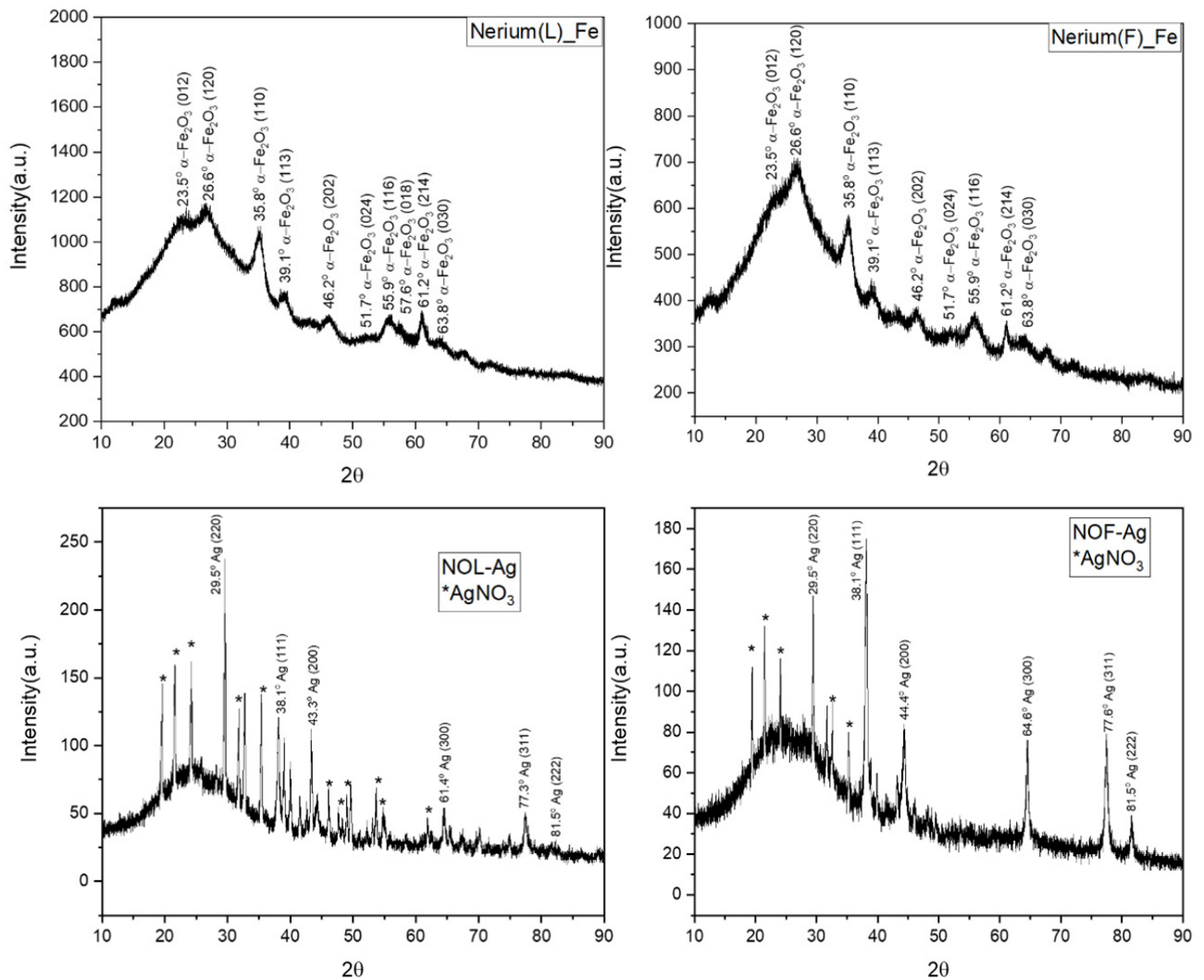


Figure 4. XRD graphs of NOL-Fe, NOF-Fe, NOL-Ag, and NOF-Ag.

and crystalline (cubic crystalline structure, $a=4.07100 \text{ \AA}$; JCPDS files no. 84-0713 and 04-0783). The obtained diffraction peaks at 2θ values of 26.50° , 36.78° , and 38.40° were assigned to (220), (111), and (111) lattice planes, respectively. Those sets of lattice planes were identical to those reported for standard silver metal (JCPDS files no. 84-0713 and 04-0783).

FTIR analysis

FTIR spectra of NOF and NOF-NPs are presented in Fig. 5. The absorption band at 3300 cm^{-1} was mainly attributed to OH vibration. The absorption peaks were assigned to the stretching vibration of C=C (1645 cm^{-1}). Compared to NOF extract's FTIR, the disappearance of the most functional group is due to the successful reduction of metal ions. Three main bands were demonstrated in the FTIR spectrum of both NOF-FeNPs and NOF-AgNPs. The presence of

OH bonds and C=O functional groups on the NOF-AgNPs and NOF-AgNPs were presented at 3244 cm^{-1} and 1633 cm^{-1} , respectively. It was reported in the literature that FeNPs exhibit a characteristic stretching Fe-O vibration peak at 576 cm^{-1} (Wang et al., 2014). For NOF-AgNPs, stretching vibrations at 631 cm^{-1} can also be attributed to the reduction of Ag^+ to Ag. In similar green synthesis studies also reported observation of reduction of Ag^+ to Ag peak at around 538 cm^{-1} (Erdogan et al., 2019). The FTIR spectrums of NOL-Ag and NOL-Fe are similar to the FTIR spectrums of NOF-Ag and NOF-Fe. Therefore, there was no need to reinterpret the NOL-Ag and NOL-Fe spectrums.

Cytotoxicity assay

NOL-AgNPs are effective in the K562 cancer cell line ($\text{IC}_{50} = 2.3 \text{ \mu M}$). However, NOF-AgNPs are variable ($\text{IC}_{50} = 10 \text{ \mu M}$). Similarly, NOF-

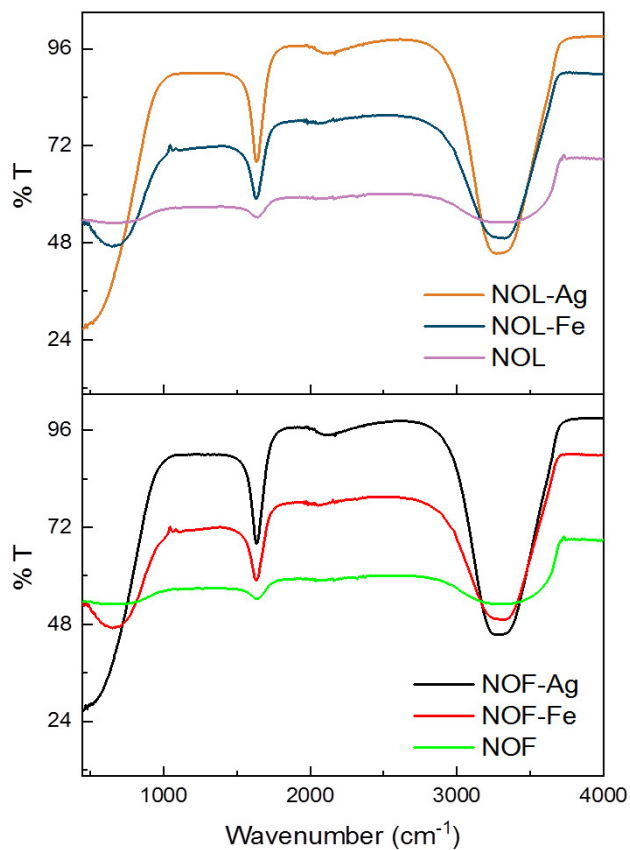


Figure 5. FTIR of NOL-Ag, NOL-Fe, NOF-Ag, NOF-Fe, and crude NOL and NOF extracts.

FeNPs (IC_{50} - 7 μ M) are more variable than the NOL-FeNPs (IC_{50} - 48 μ M). Our results suggested that NOL-Ag, NOF-Ag, NOF-Fe, and NOL-Fe are effective on the K562 cell line in low concentrations. Furthermore, we may conclude that NOF-Ag and NOF-Fe NPs have a cytotoxic effect on the K562 cell line in similar concentrations. However, NOL-Fe was cytotoxic at concentrations approximately 20 times higher than NOL-Ag (Fig. 6).

In other studies, *N. oleander* conjugated gold nanoparticles were synthesized to investigate *in vitro* anticancer activity on MCF-7 cell lines. IC_{50} values of these nanoparticles were found between 74.04 and 130.87 μ g/mL. These values are much higher than ours (Barai et al., 2018).

HUVECs were used in this study as a control. Ag and Fe NPs were not effective on HUVEC cells at the same concentrations. NOL-Ag (IC_{50} - 100 μ M), NOF-Ag (IC_{50} - 100 μ M), NOF-Fe (IC_{50} - 390 μ M), and NOL-Fe (IC_{50} - 430 μ M). The concentrations of Ag and Fe NPs, which are cytotoxic on HUVEC cells, are more than ten-fold higher compared to K562 cells. These results show that

nanoparticles are harmless to normal cells when used at low doses, which are cytotoxic to leukemia cells (Fig. 6).

Antibacterial activity

Based on the results in Table 4, the tested bacteria were able to be killed at a low concentration of $AgNO_3$ (<0.00976 mM). The green-synthesized NOL-Ag and NOF-Ag were able to inhibit bacteria including multidrug pathogens. As showed in Table 5, the MIC (mg/mL|mg/mM) values of NOL-Ag and NOF-Ag against Gram-negative bacteria were ranged from 0.019|0.039 to 0.3125|0.625 and 0.078|0.156, respectively. While the MIC (mg/mL|mg/mM) values of NOL-Ag and NOF-Ag against Gram-positive bacteria ranged from 0.078|0.156 to 0.3125|0.625 and 0.078|0.156 to 0.625|1.25, respectively. There is no significant difference observed between Gram-negative and Gram-positive bacteria including multi-resistant bacteria. The result of Fe-NPs was not given because the results were not effective.

Plant-derived essential oils and extracts have an antimicrobial effect with low toxicity and can be recommended as potential natural preservatives. According to Rios & Recio (2005), extracts can be classified as significant (MIC<100 mg/L), moderate (100<MIC \le 512 mg/L), or weak (MIC>512 mg/L) depending on their respective activities against the corresponding pathogens. An important advantage for the used metallic ions is that silver ions have relatively low toxicity to human cells while adversely affecting bacteria and fungi by different mechanisms, including binding to the thiol groups of protein and denaturing them, programmed cell death (apoptosis), and causing the DNA to be in the condensed form (Lansdown, 2006; Mohamed et al., 2020).

Several studies documented the green synthesis of AgNPs using plant extracts. Also, antimicrobial effects of AgNPs against multidrug-resistant bacteria including *E. coli*, *P. aeruginosa*, and MRSA have been studied by many researchers (Rai et al., 2012; Paredes et al., 2014; Malik et al., 2015; Kar et al., 2016; Chauhan et al., 2017; Nagababu & Rao, 2017).

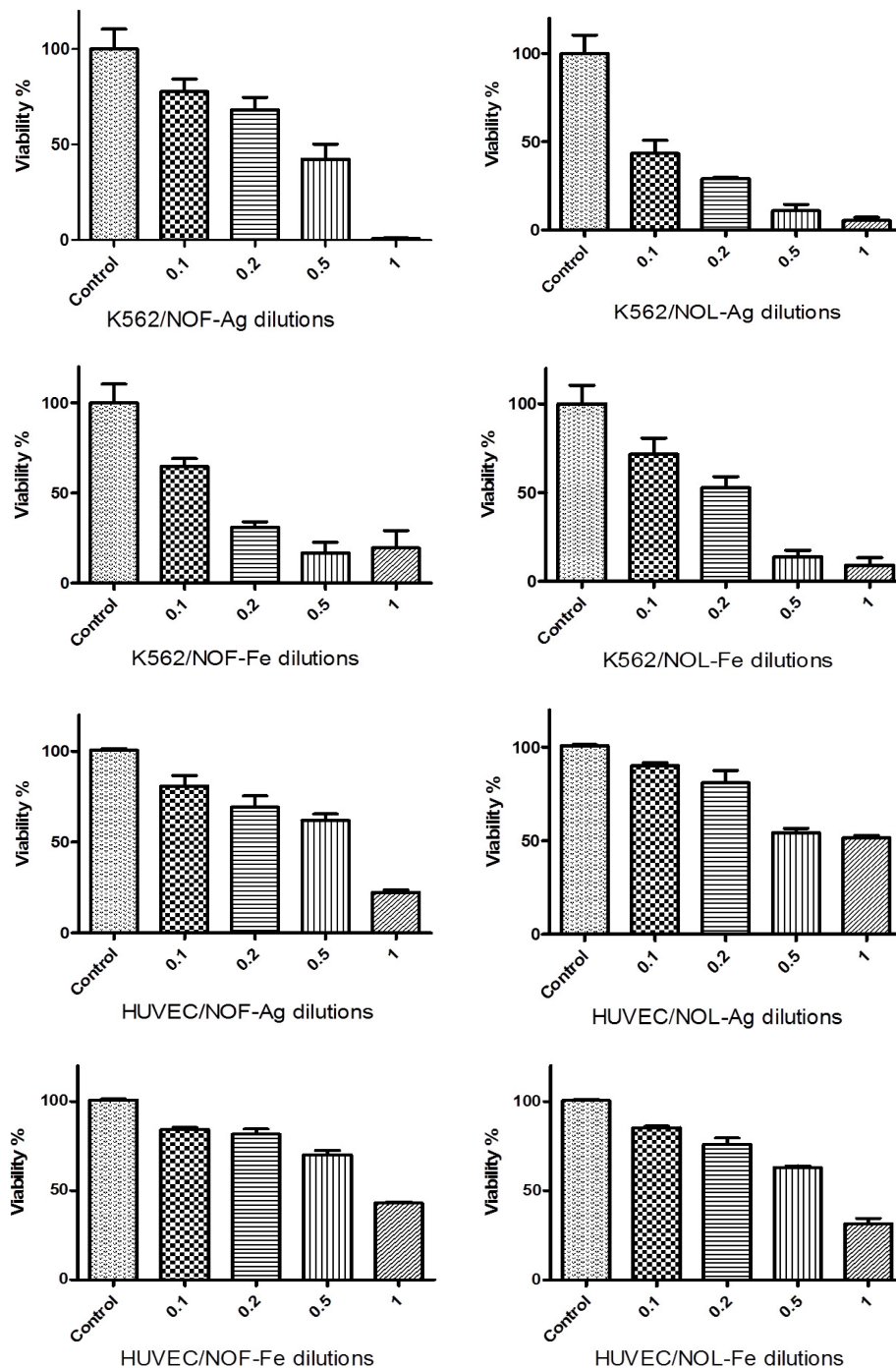


Figure 6. Cytotoxic activity of synthesized NOF-Ag, NOL-Ag, and NOF-Fe, NOL-Fe NPs against K562 and HUVEC cell lines.

Conclusions

Synthesized NPs have been successfully implemented in the fields of medicine and environmental remediation. The green synthesis of silver NPs was not only demonstrated by visual inspection and but also by performing systematic spectral techniques (UV-Vis absorption, FTIR spectroscopy,

and SEM analysis). FTIR results proved that bioactive compounds responsible for silver bio-reduction could be proteins and flavonoids presumed to act as reducing and capping agents for the silver and iron nanoparticles. This research supports the idea that the total pH of the solution should be considered when making a medical evaluation. The SEM particle size for both NPs matches with DLS

Table 5. The MICs of AgNO₃, NOL-AgNPs, and NOF-AgNPs against Gram-negative and Gram-positive bacteria.

No	Bacteria	NOL-Ag NP (mg/mL mg/mM)	AgNO ₃ (mM)	NOF-AgNP (mg/mL mg/mM)
1	<i>E. coli</i>	0.313 0.625	<0.00976	0.078 0.156
2	CRKpn	0.078 0.156	<0.00976	0.078 0.156
3	CREc	0.019 0.039	<0.00976	0.078 0.156
4	<i>S. aureus</i> (ATCC 29213)	0.156 0.313	<0.00976	0.625 1.250
5	<i>S. aureus</i> (ATCC 25923)	0.156 0.313	<0.00976	0.313 0.625
6	ICRSa	0.313 0.625	<0.00976	0.313 0.625
7	hVISA	0.313 0.625	<0.00976	0.313 0.625
8	MRSA	0.313 0.625	<0.00976	0.313 0.625
9	MR-CoNS	0.039 0.078	<0.00976	0.078 0.156
10	MR-CoNS	0.039 0.078	<0.00976	0.078 0.156
11	VREf	0.156 0.313	<0.00976	0.156 0.313
12	<i>E. faecalis</i> (ATCC 51279)	0.078 0.156	<0.00976	0.156 0.313
13	VSEf	0.039 0.078	<0.00976	0.078 0.156
14	<i>E. faecalis</i> (ATCC 29212)	0.3125 0.625	<0.00976	0.313 0.625

Note. CRKpn – clinical isolates of carbapenem-resistant *Klebsiella pneumoniae*; CREc – carbapenem-resistant *Escherichia coli*; ICRSa – inducible clindamycin-resistant *Staphylococcus aureus* BAA976-1; hVISA – hetero-resistant *S. aureus*; MRSA – clinical isolates of methicillin-resistant *S. aureus*; MR-CoNS:2 – methicillin-resistant coagulase-negative *S. aureus*; VREf – vancomycin-resistant *Enterococcus faecium*; VSEf – vancomycin-susceptible *E. faecalis*.

analysis, which was around 100 nm. The green synthesized NO-AgNPs and NO-FeNPs are cytotoxic to the human chronic myeloid leukemia cells in low concentrations and not cytotoxic to the HUVEC cell line in the same concentrations. The tested bacteria were able to be killed at a low concentration of AgNO₃ (<0.00976 mM). The green synthesized NOL-AgNPs and NOF-AgNPs were able to inhibit bacteria including multidrug pathogens. We can hypothesize here that green synthesis AgNPs can be decreased the cytotoxic effects of AgNO₃ *in vivo* and the possible use of high doses of AgNO₃ as antimicrobial drugs.

Acknowledgements

The authors would like to thank Professor Musa Mutlu Can from Istanbul University, Faculty of Science, Department of Physics, Renewable Energy and Oxide Hybrid Systems Laboratory for allowing us to use his laboratory and equipment.

References

- Al-Badrani, B. A., Rhaymah, M. S., & Al-Farwachi, M. I. (2008). Acute toxicity of *Nerium oleander*. *Iraqi Journal of Veterinary Sciences*, 22(1), 1–4. <https://doi.org/10.33899/ijvs.2008.5665>
- Arya, V. (2010). Living systems: eco-friendly nanofactories. *Digest Journal of Nanomaterials & Biostructures*, 5(1), 9–21.
- Barai, A., Paul, K., Dey, A., Manna, S., Roy, S., Bag, B., & Mukhopadhyay, C. (2018). Green synthesis of *Nerium oleander*-conjugated gold nanoparticles and study of its *in vitro* anticancer activity on MCF-7 cell lines and catalytic activity. *Nano Convergence*, 5, Article 10. <https://doi.org/10.1186/s40580-018-0142-5>
- Baytop, T. (1999). Curing with plants in Turkey, in the past and today. *Iraqi Journal of Veterinary Sciences*, 22, 1–4.
- Bharathi, V., & Shanthi, S. (2017). Green synthesis of silver nanoparticles from flower extract of *Nerium oleander* and its characterization. *World Journal of Pharmaceutical Research*, 6(6), 1410–1417.

- Bulut, G., & Tuzlaci, E. (2013). An ethnobotanical study of medicinal plants in Turgutlu (Manisa-Turkey). *Journal of Ethnopharmacology*, 149(3), 633–647. <https://doi.org/10.1016/j.jep.2013.07.016>
- Byrne, F. P., Jin, S., Paggiola, G., Petchey, T. H. M., Clark, J. H., Farmer, T. J., Hunt, A. J., McElroy, C. R., & Sherwood, J. (2016). Tools and techniques for solvent selection: green solvent selection guides. *Sustainable Chemical Processes*, 4, Article 7. <https://doi.org/10.1186/s40508-016-0051-z>
- Chaudhary, K. K., Prasad, D., Sandhu, B., & Chaudhary, K. (2015). Preliminary pharmacognostic and phytochemical studies on *Nerium oleander* Linn. (white cultivar). *Journal of Pharmacognosy and Phytochemistry*, 4, 185–188.
- Chauhan, S., Singh, M., Thakur, A., & Dogra, M. S. (2017). Antibacterial activity of *Nerium indicum* against some Gram positive bacterial species. *International Journal of Drug Research and Technology*, 3(1), 8–11.
- CLSI. (2018). *M100 – Performance standards for antimicrobial susceptibility testing*, 28th ed. Clinical and Laboratory Standards Institute.
- Erdemoglu, N., Küpeli, E., & Yeşilada, E. (2003). Anti-inflammatory and antinociceptive activity assessment of plants used as remedy in Turkish folk medicine. *Journal of Ethnopharmacology*, 89(1), 123–129. [https://doi.org/10.1016/S0378-8741\(03\)00282-4](https://doi.org/10.1016/S0378-8741(03)00282-4)
- Erdogan, O., Abbak, M., Demirbolat, G.M., Birtekocak, F., Aksel, M., Pasa, S., & Cevik, O. (2019). Green synthesis of silver nanoparticles via *Cynara scolymus* leaf extracts: the characterization, anticancer potential with photodynamic therapy in MCF7 cells. *PLOS ONE*, 14, Article e0216496. <https://doi.org/10.1371/journal.pone.0216496>
- Fedlheim, D. L., & Foss, C. A. (2001). *Metal nanoparticles: synthesis, characterization, and applications*. CRC Press.
- Gürdal, B., & Kültür, Ş. (2013). An ethnobotanical study of medicinal plants in Marmaris (Muğla, Turkey). *Journal of Ethnopharmacology*, 146(1), 113–126. <https://doi.org/10.1016/j.jep.2012.12.012>
- Harborne, A. J. (1998). *Phytochemical methods – a guide to modern techniques of plant analysis*. Springer science & business media.
- Kar, D., Bandyopadhyay, S., Dimri, U., Mondal, D. B., Nanda, P. K., Das, A. K., Batabyal, S., Dandapat, P., & Bandyopadhyay, S. (2016). Antibacterial effect of silver nanoparticles and capsaicin against MDR-ESBL producing *Escherichia coli*: an *in vitro* study. *Asian Pacific Journal of Tropical Disease*, 6(10), 807–810. [https://doi.org/10.1016/S2222-1808\(16\)61135-0](https://doi.org/10.1016/S2222-1808(16)61135-0)
- Kiran, C., & Prasad, D. N. (2014). A review on *Nerium oleander* Linn. (Kaner). *International Journal of Pharmacognosy and Phytochemical Research*, 6, 593–597.
- Lansdown, A. B. (2006). Silver in health care: antimicrobial effects and safety in use. In: U.-C. Hipler & P. Elsner (Eds), *Biofunctional textiles and the skin* (pp. 17–34). Karger Publishers. <https://doi.org/10.1159/000093928>
- Malik, R., Bokhari, T. Z., Siddiqui, M. F., Younis, U., Hussain, M. I., & Khan, I. A. (2015). Antimicrobial activity of *Nerium oleander* L. and *Nicotiana tabacum* L.: a comparative study. *Pakistan Journal of Botany*, 47(4), 1587–1592.
- Mohamed, D. S., El-Baky, R. M. A., Sandle, T., Mandour, S. A., & Ahmed, I. F. (2020). Antimicrobial activity of silver-treated bacteria against other multi-drug resistant pathogens in their environment. *Antibiotics*, 9(4), Article 181. <https://doi.org/10.3390/antibiotics9040181>
- Mosmann, T. (1983). Rapid colorimetric assay for cellular growth and survival: application to proliferation and cytotoxicity assays. *Journal of Immunological Methods*, 65(1–2), 55–63. [https://doi.org/10.1016/0022-1759\(83\)90303-4](https://doi.org/10.1016/0022-1759(83)90303-4)
- Nagababu, P., & Rao, V. U. (2017). Pharmacological assessment, green synthesis and characterization of silver nanoparticles of *Sonneratia apetala* Buch.-Ham. leaves. *Journal of Applied Pharmaceutical Science*, 7(8), 175–182. <https://doi.org/10.7324/japs.2017.70824>
- Paredes, D., Ortiz, C., & Torres, R. (2014). Synthesis, characterization, and evaluation of antibacterial effect of Ag nanoparticles against *Escherichia coli* O157:H7 and methicillin-resistant *Staphylococcus aureus* (MRSA). *International Journal Of Nanomedicine*, 9(1), 1717–1729. <https://doi.org/10.2147/IJN.S57156>
- Pathak, S., Multani, A. S., Narayan, S., Kumar, V., & Newman, R. A. (2000). Anvirzel™, an extract of *Nerium oleander*, induces cell death in human but not murine cancer cells. *Anti-Cancer Drugs*, 11, 455–463. <https://doi.org/10.1097/00001813-200007000-00006>
- Rai, M. K., Deshmukh, S. D., Ingle, A. P., & Gade, A. K. (2012). Silver nanoparticles: the powerful nanoweapon against multidrug-resistant bacteria. *Journal of Applied Microbiology*, 112(5), 841–852. <https://doi.org/10.1111/j.1365-2672.2012.05253.x>
- Ríos, J. L., & Recio, M. C. (2005). Medicinal plants and antimicrobial activity. *Journal of Ethnopharmacology*, 100(1–2), 80–84. <https://doi.org/10.1016/j.jep.2005.04.025>

- Rubini, S., Rossi, S. S., Mestria, S., Odoardi, S., Chendi, S., Poli, A., Merialdi, G., Andreoli, G., Frisoni, P., Gaudio, R. M., Baldisserotto, A., Buso, P., Manfredini, S., Govoni, G., Barbieri, S., Centelleghè, C., Corazzola, G., Mazzariol, S., & Locatelli, C. A. (2019). A probable fatal case of oleander (*Nerium oleander*) poisoning on a cattle farm: a new method of detection and quantification of the oleandrin toxin in rumen. *Toxins*, 11(8), Article 442. <https://doi.org/10.3390/toxins11080442>
- Sağiroğlu, M., Dalgıccedil, S., & Toksoy, S. (2013). Medicinal plants used in Dalaman (Muğla), Turkey. *Journal of Medicinal Plants Research*, 7, 2053–2066. <https://doi.org/10.5897/JMPR2013.2590>
- Santhi, R. (2011). Phytochemical screening of *Nerium oleander* leaves and *Momordica charantia* leaves. *International Research Journal of Pharmacy*, 2, 131–135.
- Saranya, S., Archana, D., & Santhy, K. (2017). Antimicrobial and antioxidant effects of *Nerium oleander* flower extracts. *International Journal of Current Microbiology and Applied Sciences*, 6(5), 1630–1637. <https://doi.org/10.20546/ijemas.2017.605.178>
- Sikarwar, M. S., Patil, M. B., Kokate, C. K., Sharma, S., & Bhat, V. (2009). Antidiabetic activity of *Nerium indicum* leaf extract in alloxan-induced diabetic rats. *Journal of Young Pharmacists*, 1(4), 340–345.
- Singhal, K. G., & Gupta, G. D. (2012). Hepatoprotective and antioxidant activity of methanolic extract of flowers of *Nerium oleander* against CCl₄-induced liver injury in rats. *Asian Pacific Journal of Tropical Medicine*, 5(9), 677–685. [https://doi.org/10.1016/S1995-7645\(12\)60106-0](https://doi.org/10.1016/S1995-7645(12)60106-0)
- Turan, N., Akgün-Dar, K., Kuruca, S. E., Kiliçaslan-Ayna, T., Seyhan, V. G., Atasever, B., Meriçli, F., & Carin, M. (2006). Cytotoxic effects of leaf, stem and root extracts of *Nerium oleander* on leukemia cell lines and role of the p-glycoprotein in this effect. *Journal of Experimental Therapeutics & Oncology*, 6(1), 31–38.
- Tyler, V. E. (1993). *Phytomedicines in Western Europe: potential impact on herbal medicine in the United States*. ACS Publications.
- Wang, Z., Liu, Y., Huang, B., Dai, Y., Lou, Z., Wang, G., Zhang, X., & Qin, X. (2014). Progress on extending the light absorption spectra of photocatalysts. *Physical Chemistry Chemical Physics*, 16(7), 2758–2774. <https://doi.org/10.1039/C3CP53817F>
- Wong, S. K., Lim, Y. Y., Abdullah, N. R., & Nordin, F. J. (2011). Antiproliferative and phytochemical analyses of leaf extracts of ten Apocynaceae species. *Pharmacognosy Research*, 3(2), 100–106. <https://doi.org/10.4103/0974-8490.81957>
- Zibbu, G., & Batra, A. (2010). A review on chemistry and pharmacological activity of *Nerium oleander* L. *Journal of Chemical and Pharmaceutical Research*, 2, 351–358.

Зелений синтез та характеристика наночастинок срібла та заліза отриманих з використанням екстрактів *Nerium oleander* та їх антибактеріальна та протипухлинна активність

Шаліма Шавуті¹, Часан Байрам², Ахмет Беятлі³, Ішак Афшін Каріпер⁴, Исик Неслішах Коркут¹, Зеррін Акташ⁵, Мустафа Орал Онцюл⁶, Серап Ердем Куруца¹

¹ Кафедра фізіології, медичний факультет Стамбульського університету, вул. Тургута Озала Міллета, Стамбул, 34093, Туреччина

² Лабораторія відновлюваних джерел енергії та оксидних гібридних систем, кафедра фізики, факультет природничих наук Стамбульського університету, вул. Шехзадебаші, Стамбул, 34134, Туреччина

³ Кафедра лікарських та ароматичних рослин Гамідійського професійно-технічного училища охорони здоров'я Університету медико-санітарних наук, вул. Тібійє, 38, Стамбул, 34668, Туреччина

⁴ Педагогічний факультет університету Ерджієс, Енідоган Махаллесі, вул. Турхан Байтоп Сокак, 1, Кайсері, 38280, Туреччина

⁵ Кафедра мікробіології, медичний факультет Стамбульського університету, вул. Тургута Озала Міллета, Стамбул, 34093, Туреччина

⁶ Кафедра інфекційних захворювань, медичний факультет Стамбульського університету, вул. Тургута Озала Міллета, Стамбул, 34093, Туреччина

Лікарські рослини можуть використовуватися як відновники при одержанні наночастинок металів шляхом зеленого синтезу. Отримані наночастинки характеризуються хіміотерапевтичним та протиінфекційним властивостям природних сполук. Зокрема, у цій праці йдеться про зелений синтез наночастинок срібла та заліза з використанням екстрактів листя та квіток *Nerium oleander*, а також аналізується їх властивості як протипухлинних та протимікробних засобів. Повідомляється про особливості виготовлення наночастинок загалом та структурну характеристику наночастинок срібла та заліза зокрема. Формування наночастинок досліджено за допомогою сканувальної електронної мікроскопії та енергодисперсійної рентгенівської спектроскопії, UV-Vis та інфрачервоної спектроскопії з перетворенням Фур'є (FTIR). Окрім того, також було досліджено поверхневим заряд, розміри і розподілом наночастинок за допомогою DLS аналізу. Зелений синтез наночастинок срібла та заліза з використанням *N. oleander* показав різні рівні селективної цитотоксичності щодо K562 (клітини хронічної мієлоїдної лейкемії людини) у низьких концентраціях і не був цитотоксичним для HUVEC (ендотеліальні клітини пупкової вени людини) у тих же концентраціях. Наночастинок срібла виявляли антибактеріальну активність по відношенню до мультирезистентних патогенів, тоді як наночастинок заліза не виявляли такої активності. Результати цього дослідження підтверджують потенціал використання наночастинок зеленого синтезу у різних сферах біомедицини та фармацевтики в майбутньому.

Ключові слова: *Nerium oleander*, зелений синтез, Ag-наночастинок, Fe-наночастинок, клітинна цитотоксичність, антибактеріальний ефект